

Effect of heavy doping in SnO₂:F films

CHITRA AGASHE, S. S. MAJOR

Department of Physics, Indian Institute of Technology, Powai, Bombay 400 076, India

Thin films of fluorine-doped tin dioxide (SnO₂:F) were deposited by a spray pyrolysis technique on soda lime glass substrates. Structural and electronic transport properties of the films deposited with different doping levels of fluorine (zero to 350 at %) were investigated. X-ray diffraction technique and Hall effect measurements were used for this work. Growth rate of the films was considerably affected by doping, specially at higher doping levels. The films were polycrystalline and preferentially oriented along [200]. This preferred growth played a dominant role in determining the transport properties. Notably the charge carrier mobility was directly governed by this preferred growth. The electrical conductivity was totally governed by the carrier concentration. The respective changes in carrier concentration were used to suggest the site selection of the fluorine dopant in the SnO₂ lattice.

1. Introduction

Thin films of nonstoichiometric metal oxides, such as SnO₂, In₂O₃, ZnO and their doped forms, possess high visible transparency and high electrical conductivity [1–4]. The simultaneous occurrence of these properties makes these films extremely suitable for use as optical window and/or as an electrode in solar energy conversion devices and various other applications [1]. Undoped and doped tin dioxide films have been developed as a very effective transparent conducting coating. Among the several cationic and anionic dopants, fluorine has been observed to be the most effective dopant probably due to its closer ionic size to that of oxygen.

The present work is part of a development of SnO₂:F thin films with high performance as transparent conducting coatings using a spray pyrolysis technique. The films were deposited with very high dopant levels. Other process parameters were kept constant at their optimum values [5]. From the dependence of the carrier concentration on the doping level, some predictions could be made about site selection by dopants.

2. Experimental procedure

A spray pyrolysis technique was employed to deposit SnO₂:F films. Doping was achieved by adding an appropriate amount of NH₄F to the precursor solution of 0.2 M concentration (SnCl₄·5H₂O dissolved in deionized water and methanol with a volume ratio 1:9). Soda lime glass substrates were used. Other process parameters were kept constant as given in an earlier work [5]. The extent of doping in solution was varied from zero to 350 at %.

Spectrophotometric measurements were carried out using Shimadzu UV-160 A double beam spectrophotometer. Film thickness was calculated from

interference patterns observed in the visible region of “transmission versus wavelength” curves [6]. Structural properties were investigated by X-ray diffraction techniques. Low angle and bulk X-ray diffractograms were taken using Rigaku Rotaflex (Ru 200B) and Philips (PW 1840) diffractometers, with CuK_α (λ = 0.1542 nm) radiation. The relative prominence of preferred orientation [hkl] with respect to other observed orientations was expressed in terms of a parameter *RP* [hkl] defined as,

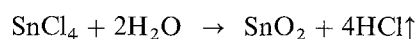
$$RP(hkl) = \frac{I(hkl)}{\sum I(hkl)} \quad (1)$$

Here, *I*(hkl) is the relative intensity of a plane (hkl) as observed in the X-ray diffractogram. The grain size was derived using the Debye–Scherrer formula [7]. The electronic transport properties were determined by performing Hall measurements using van der Pauw geometry [8].

3. Results and discussion

Fig. 1 shows the dependence of film growth rate on the doping level of fluorine. In the case of undoped SnO₂ films, the growth rate is about 2.2 nm s⁻¹. Doping the films with fluorine up to 50 at % did not affect the growth rate. Further doping resulted in a reduction in the growth rate. These results show that at higher doping levels the reaction processes which control the growth kinetics are considerably affected by fluorine. To understand this one needs to discuss how the film is grown from the spray solution.

In the present case, the hydrated SnCl₄ decomposes which results in the formation of SnO₂ and HCl vapour according to the equation,



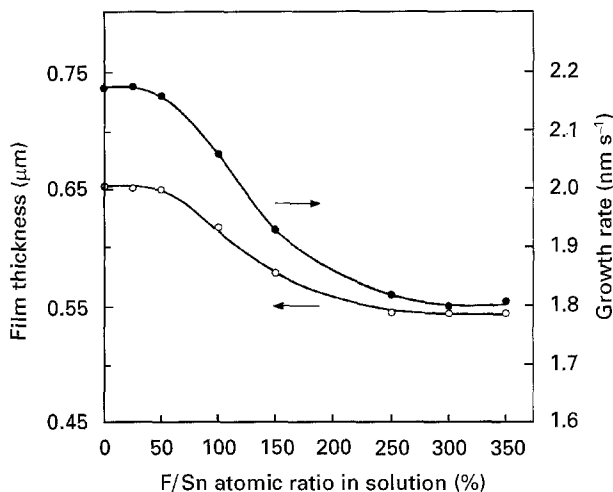
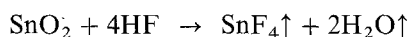


Figure 1 Dependence of growth rate on doping level for fluorine-doped SnO₂ films.

Simultaneously, the decomposition of ammonium fluoride takes place according to the equation,



The decomposition temperature of ammonium fluoride is quite low. Therefore it takes place almost instantaneously and forms a cloud of HF in the vicinity of the growing SnO₂ film. There is the possibility of a chemical reaction between the growing SnO₂ film and the haloacid. In this case the following reaction would take place,



and this would obviously result in retarding the formation of the layers. Applying the law of mass action to these processes one can notice that the externally added dopant increases the rate of backward reaction through the fourth power dependence of HF concentration. Hence, the rate of deposition of the SnO₂ film will be determined by the competition between the rate of formation of SnO₂ and the rate of etching of SnO₂ by HF.

Perusal of bond strengths of haloacids indicates that HF is the weakest acid with a bond dissociation energy = 569.0 kJ mol⁻¹. Effectively, one observes a comparable drop in the growth rate at significantly higher doping levels. This drop in growth rate suggests the formation of some SnF_x-type compounds which will make Sn gradually unavailable for SnO₂ deposition.

Fig. 2 shows the effect of fluorine doping on the structural properties of SnO₂ films. It is quite clear from this figure that irrespective of the doping level, the films are highly oriented along [200]. Presence of other orientations such as [110], [211], [310], [301] and [321] also have been detected but with substantially lower intensities. Due to this preferred growth along [200], the orientational properties of the film as a whole have been expressed in terms of the parameter *RP*(200) defined in the previous section.

Fig. 3 gives the effect of doping on *RP*(200). As compared to undoped films, initially at the lower doping levels, *RP*(200) decreases. This is followed by

an increase at higher doping levels. These results can be explained in the following manner.

The initial decrease in *RP*(200) may be associated with the incorporation of dopants at oxygen sites or vacancies. Growth rate of the film being a function of the doping level, also plays an important role in determining the preferential growth. It is a general observation that as the growth rate decreases, high atomic density planes become preferentially developed [9]. On these grounds, it can be justified that for reduced growth rates, as observed for films with higher doping level, the high density planes, in the present case (110) and (211), will be preferentially grown reducing *RP*(200) as seen in Fig. 3. For still higher doping levels, one expects further enhancement in the intensity of the high density planes. But along with this the intensity of [200] also is enhanced, thereby increasing *RP*(200).

The grain size dependence on dopant concentration is very weak (Fig. 4). First it rises slightly and then tapers off. We believe that here the grain size is mainly a function of the number of nuclei available at the time of deposition. If these increase beyond a certain limit, then the grain size will decrease. It is quite logical to expect that here nucleating centres are mainly provided by the partially hydrolysed SnCl₄ species, present in colloidal form, and the concentration of Sn-containing species, itself being high, there is not a significant change in the grain size with dopant level.

The electrical properties namely the conductivity, σ , carrier concentration n and carrier mobility, μ , are observed to follow a systematic trend. Fig. 5a shows the variation in σ with doping level. This variation is a result of the respective changes in n and μ given in Fig. 5b and c. The similar variations of σ and n with doping level show that σ is mainly determined by the carrier concentration. This is not surprising since doped tin dioxide is a degenerate semiconductor and therefore the carrier concentration has a preponderance over mobility. Initially, at very low doping levels, there is a reduction in the carrier concentration as well as in conductivity. Then, the carrier concentration increases monotonically up to a doping level of 250 at % and appears to nearly saturate thereafter. This trend in n (and also in σ) can be explained with the aid of the following model.

The undoped films contain some oxygen vacancies because the films are deposited using methanol as a solvent. Methanol decomposes at the deposition temperature into CO and H₂. Even admitting the fact that the deposition is carried out in air, the conditions in the immediate vicinity of the growing film are likely to be deficient in oxygen because the decomposition products of methanol will take a finite time to diffuse away from the surface of the growing layer of the film. Also methanol flux is constant in all cases. Therefore one can make the following statements about the undoped films:

- (i) the undoped film is most likely to have oxygen vacancies;
- (ii) it is quite possible that some of these oxygen vacancies may have been filled by residual chlorine

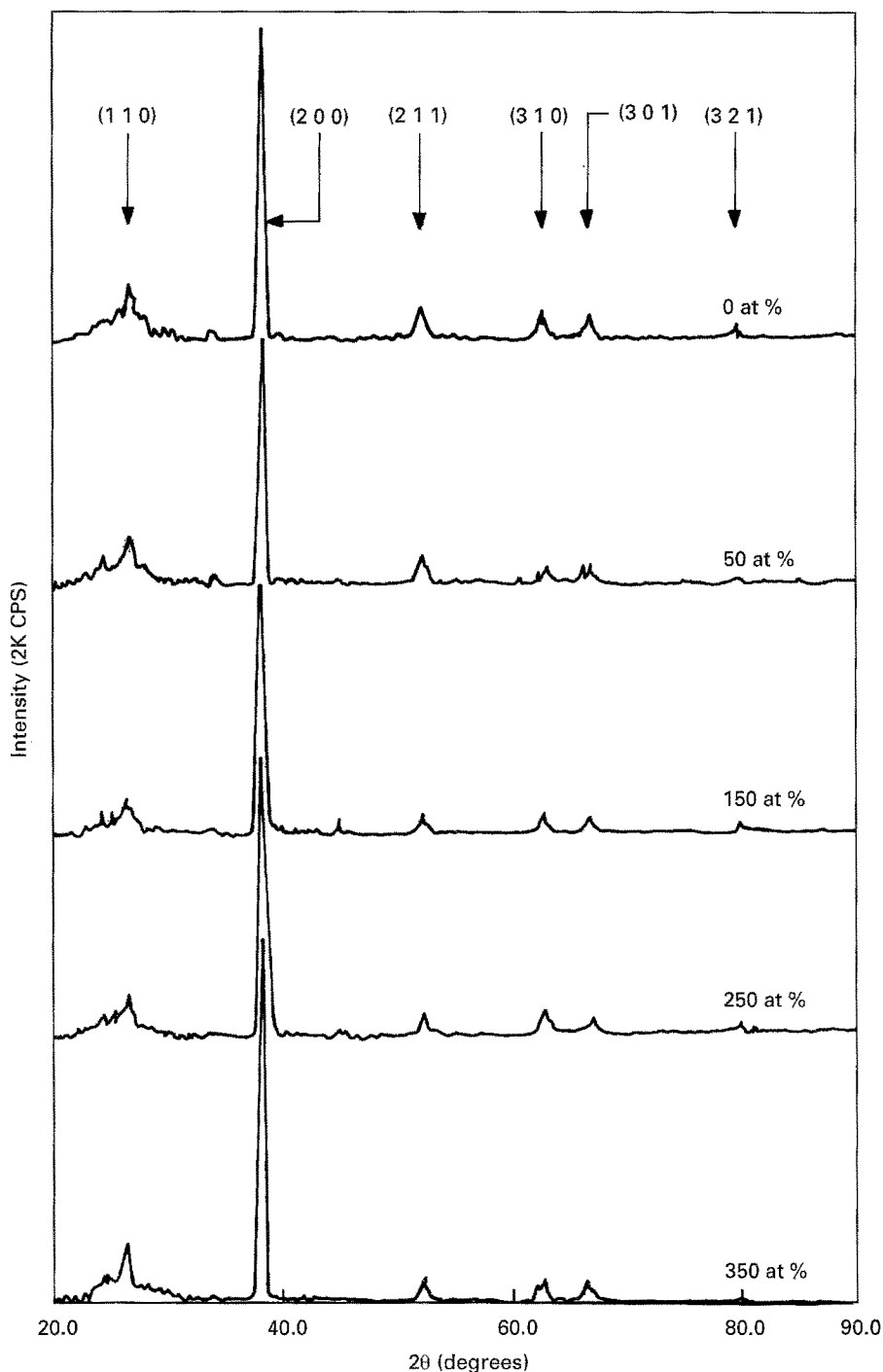


Figure 2 X-ray diffractograms of $\text{SnO}_2:\text{F}$ films with different doping levels.

from the precursor solution containing $\text{SnCl}_4 \cdot 5\text{H}_2\text{O}$; and

(iii) as a result of excess concentration of the tin-containing species ($\text{SnCl}_4 \cdot 5\text{H}_2\text{O}$) in the precursor solution, tin atoms may get incorporated interstitially as well.

As the fluorine doping commences, the respective change in n will depend upon the lattice site where the dopant becomes incorporated at different doping levels. If the dopant is incorporated at an oxygen vacancy, one expects a drop in the carrier concentration. If it replaces oxygen, an increase in the carrier concentration will be observed. In the case of excess and hence interstitial incorporation, fluorine being an

electron acceptor, again a drop in n will be observed. Therefore, the initial drop in carrier concentration can be attributed to the filling of oxygen vacancies. The lattice will become highly distorted around such vacancies and the dopant will prefer to fill these oxygen vacancies first. Once a comparable number of oxygen vacancies are filled, the dopant will enter the SnO_2 lattice substitutionally. However, the substitution is decided by ionic size and charge of the dopant. In the case of $\text{SnO}_2:\text{F}$ films, fluorine appears to be the most favoured substituent because, (a) its ionic size (F^- : 0.133 nm) very closely matches with that of oxygen (O^{2-} : 0.132 nm), (b) the energy of the Sn-F bond ($\sim 26.75 \text{ D}^\circ/\text{kJ mol}^{-1}$) is comparable to that of the Sn-O bond ($\sim 31.05 \text{ D}^\circ/\text{kJ mol}^{-1}$) and (c) since the

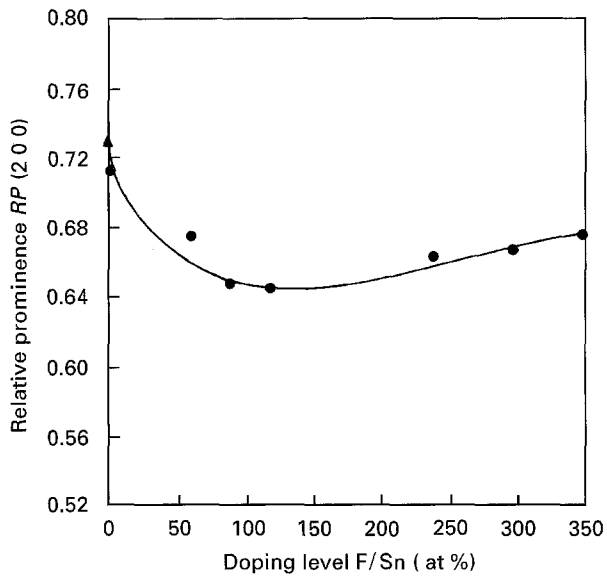


Figure 3 Relative prominence of [200] orientation for $\text{SnO}_2\text{:F}$ films. \blacktriangle Undoped SnO_2 film.

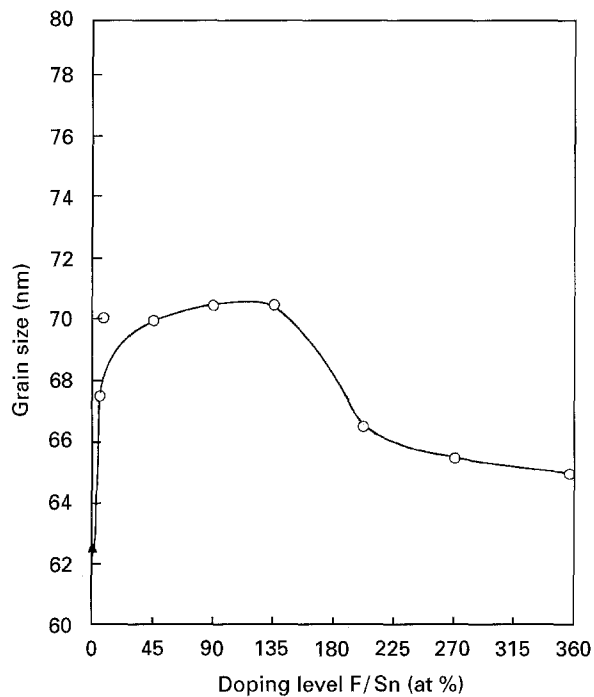
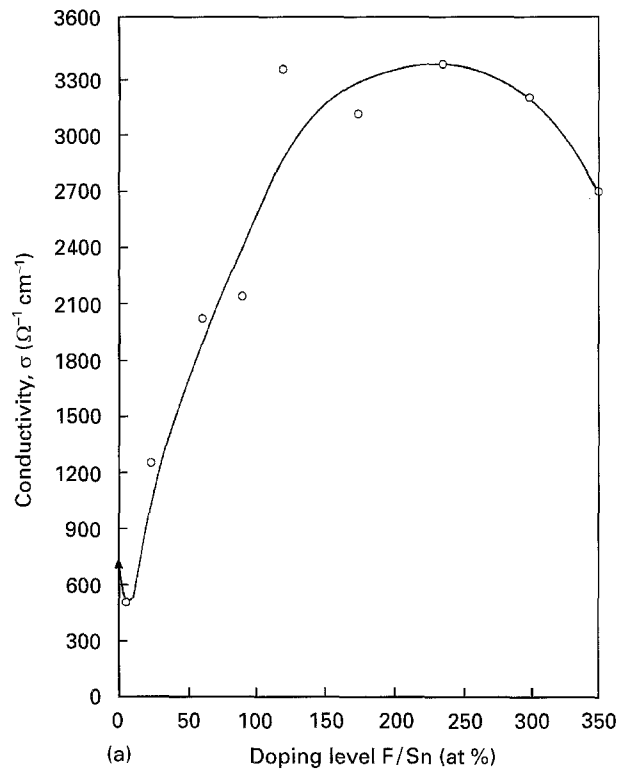


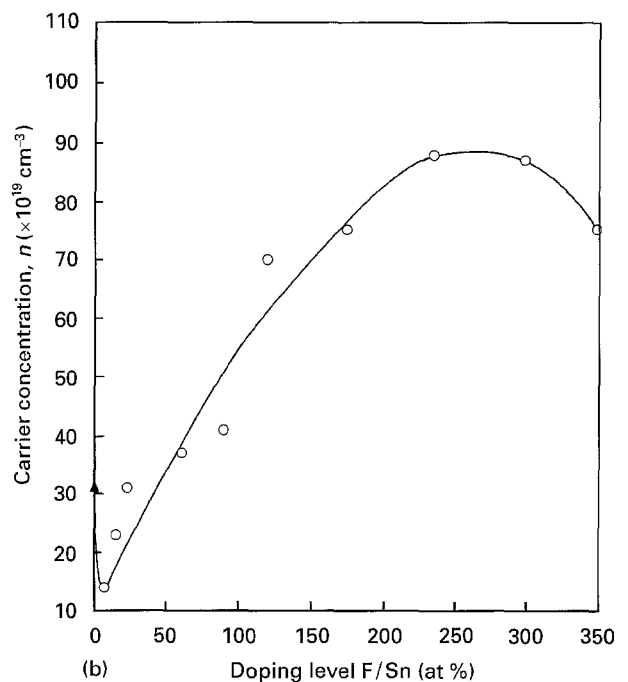
Figure 4 Dependence of grain size on doping level in $\text{SnO}_2\text{:F}$ films. \blacktriangle Undoped SnO_2 film.

charge on the fluorine ion is only half that of the charge on the oxygen ion, the Coulomb forces that bind the lattice together are reduced. Thus, geometrically the lattice is nearly unable to distinguish between fluorine and oxygen ions. The increase in carrier concentration following the initial reduction suggests the substitutional incorporation at oxygen sites. But this does not proceed much further. The reduction in n for higher doping levels clearly suggests a probable interstitial incorporation of the dopant taking place in the SnO_2 lattice.

The carrier mobility in undoped SnO_2 films is $\sim 14 \text{ cm}^2 \text{ V}^{-1} \text{ s}^{-1}$. Fig. 5 shows that as doping commences, there is a rise in mobility followed by a fall. The higher mobility value is because of the preferential



(a) Doping level F/Sn (at %)



(b) Doping level F/Sn (at %)

Figure 5 (a) Variation of conductivity with doping level for $\text{SnO}_2\text{:F}$ films. (b) Variation of carrier concentration with doping level for $\text{SnO}_2\text{:F}$ films. (c) Variation of carrier mobility with doping level for $\text{SnO}_2\text{:F}$ films. \blacktriangle Undoped SnO_2 film.

growth along [200]. The carrier mobility in undoped films is comparatively lower because of the lattice distortion originating from the oxygen vacancies. As fluorine doping begins, the dopant occupies the vacant sites which thereby reduces the lattice disorder. As a result, one observes a significant improvement in carrier mobility due to F doping. The increase in the grain size observed in this region reduces the effect of grain boundary scattering. But for very high doping levels, a reduction in carrier mobility is observed

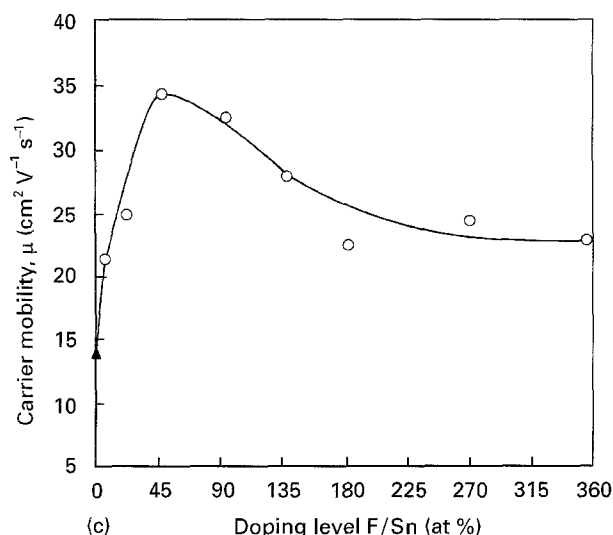


Figure 5 continued.

which is due to ionized impurity scattering. The presence of ionized impurity scattering was confirmed using the Johnson and Lark-Horovitz relation [10].

4. Conclusions

The effect of fluorine doping on the physical properties of sprayed SnO_2 films was studied in detail. It was observed that the preferred growth of the films remained along [100] direction in all cases. The strength of HF played a vital role in determining the growth rate. The grain size was slightly affected by doping. As a result, the carrier mobility showed small changes. The conductivity was totally governed by the

carrier concentration. Based on the variation in carrier concentration some predictions could be made regarding the site selection by the dopants.

Acknowledgement

One of the authors, Chitra Agashe acknowledges the financial support from the CSIR, New Delhi during the Pool Officership.

References

1. K. L. CHOPRA, S. MAJOR and D. K. PANDYA, *Thin Solid Films* **102** (1983) 1.
2. E. SHANTHI, V. DUTTA, A. BANERJEE and K. L. CHOPRA, *J. Appl. Phys.* **51** (1980) 6243.
3. J. P. UPADHYAY, S. R. VISHWAKARMA and H. C. PRASAD, *Thin Solid Films* **169** (1989) 195.
4. H. HAITJEMA and G. F. WOERLEE, *ibid.* **169** (1989) 1.
5. C. AGASHE, M. G. TAKWALE, V. G. BHIDE, S. MAHAMUNI and S. K. KULKARNI, *J. Appl. Phys.* **70** (1991) 7382.
6. J. C. MANIFACIER, J. P. FILLARD and J. M. BIND, *Thin Solid Films* **77** (1981) 67.
7. B. D. CULLITY, "Elements of X-ray Diffraction" (Addison-Wesley, Massachusetts, 1956) p. 99.
8. W. R. RUNYAN, "Semiconductor Measurements and Instrumentation" (McGraw Hill, Kogakusha Ltd., Tokyo, 1975) p. 137.
9. D. K. MURTI and T. L. BLUHM, *Thin Solid Films* **87** (1982) 57.
10. V. A. JOHNSON and K. LARK-HOROVITZ, *Phys. Rev.* **71** (1947) 374.

Received 22 February

and accepted 6 November 1995